A&A 372, 477–494 (2001)
DOI: 10.1051/0004-6361:20010441

Astronomy & Astrophysics

Photometric study of the double cluster h & χ Persei*

A. Marco and G. Bernabeu

Dpto. de Física, Ingeniería de Sistemas y Teoría de la Señal, Universidad de Alicante, Aptdo. de Correos 99, 03080, Alicante, Spain

Received 20 July 2000 / Accepted 28 January 2001

Abstract. We present $uvby\beta$ CCD photometry of the central region of the double cluster h & χ Persei. We identify ≈350 stars, of which 214 were not included in Oosterhof's catalogue. Our magnitude limit $V = 16.5$ allows us to reach early F spectral type and obtain very accurate fits to the ZAMS. We derive reddening values of $E(b-y) = 0.44 \pm 0.02$ for h Persei and $E(b-y) = 0.39 \pm 0.05$ for χ Persei. From the ZAMS fitting, we derive distance moduli $V_0 - M_V = 11.66 \pm 0.20$ and $V_0 - M_V = 11.56 \pm 0.20$ for h and χ Persei respectively. These values are perfectly compatible with both clusters being placed at the same distance and having identical reddenings. The shift in the main-sequence turnoff and isochrone fitting, however, show that there is a significant age difference between both clusters, with the bulk of stars in h Persei being older than χ Persei. There is, however, a significant population of stars in h Persei which are younger than χ Persei. All this argues for at least three different epochs of star formation, corresponding approximately to $\log t = 7.0, 7.15$ and $7.3^{\star\star}$.

Key words. techniques: photometric – Galaxy: open clusters and associations: individual: h Persei, χ Persei – stars: evolution – emission-line, Be–formation

1. Introduction

Photometric studies of open clusters are extremely useful to determine the physical properties of star members. Even though modern spectroscopic techniques allow the observation of large numbers of stars in a relatively short time, the stellar population of most clusters is still too vast for an in-depth study. Among photometric systems, the $uvby$Hβ system is the most appropriate for the study of early-type stars, since it has been designed to provide accurate measurements of their intrinsic properties.

This is the first in a series of papers dedicated to the study of the B-star population of Galactic open clusters. B-type stars are sufficiently bright to allow very accurate narrow-band photometry and at the same time numerous enough to provide a statistically significant population (unlike the brighter but very rare O-type star). The double cluster h & χ Persei is one of the richest young open clusters accessible from the Northern hemisphere, and therefore it is well documented in the literature. An extensive photographic study was carried out by Oosterhoff (1937); MK spectral types for cluster members were determined by Bidelman (1943), Johnson & Morgan (1955), Schild (1965, 1966, 1967) and others; optical photometry in various systems was carried out by Johnson & Morgan (1955), Wildey (1964), Schild (1965), Crawford et al. (1970b), Waelkens et al. (1990), and others; infrared photometry was obtained by Mendoza (1967) and Tapia et al. (1984). A study of the membership probability of 3086 stars brighter than $B = 15.5$ magnitudes within an area of 50 arcmin radius centered on h & χ Persei was carried out by Muminov (1983) on the basis of proper motion and photometric $(V-(B-V); V-(U-V); (U-B)-(B-V))$ criteria. There is no general agreement on the distance moduli and the ages of both clusters. Crawford et al. (1970b) conclude, on the base of $uvby\beta$ photometry, that both clusters have nearly the same age and distance, the distance modulus being 11.4 ± 0.4 mag. Balona & Shobbrook (1984), however, correct this value for evolutionary effects and adopt a distance modulus of 11.16 for both clusters. On the other hand, Tapia et al. (1984) find confirmation of a previous suggestion by Schild (1967) that h Persei is younger and closer than χ Persei, with distance moduli of 11.7 and 12.0, respectively. Doom et al. (1985) show that in the OB association Per OB1 the low mass stars formed first, the most massive stars being

Send offprint requests to: A. Marco,
e-mail: amparo@astronomia.disc.ua.es

* Based on observations obtained with the Jacobus Kapteyn Telescope operated on the island of La Palma by the Isaac Newton Group, in the Spanish Observatorio Roque de los Muchachos of the Instituto de Astrofísica de Canarias.

** Tables 2, 8 and 9 are only available in electronic form at the CDS via anonymous ftp to
cdsarc.u-strasbg.fr (130.79.128.5) or via
http://cdsweb.u-strasbg.fr/cgi-bin/qcat?J/A+A/372/477

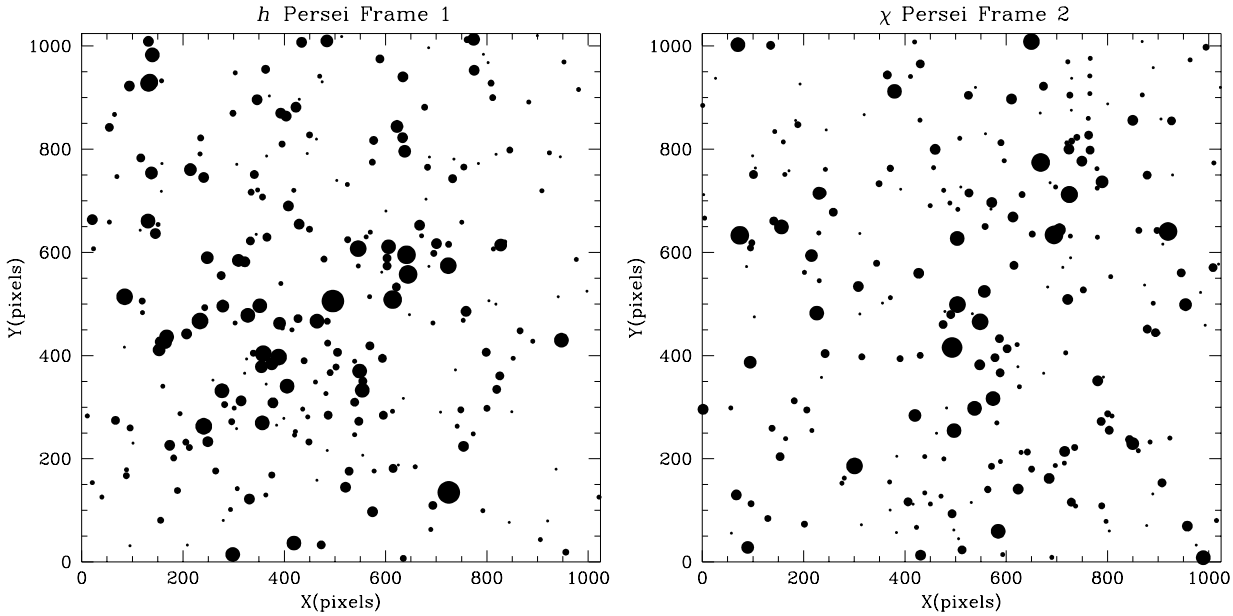

Fig. 1. a),b). Schematic maps of the observing region in NGC 884 and NGC 869. The size of the dots represents relative brightness of stars in the field. North is down and East left in all fields.

Table 1. Log of the observations taken at the 1.0-m JKT on December 11th and December 22nd 1997 for two frames.

Cluster	Frame	Central Star	Coordinates (1950)
h Persei	#1	1057	$\alpha = 2$h 15m 32.67s $\delta = +56°54'20''.49$
χ Persei	#2	2227	$\alpha = 2$h 18m 27.70s $\delta = +56°55'02''.08$
Filter	Exposure Times (s)		
	$[V \leq 10]$		$[V \geq 16]$
u	60	300	1200
v	22	110	450
b	7	40	150
y	6	30	120
$H\beta_{narrow}$	50	250	1000
$H\beta_{wide}$	6	30	120

(10−20) Myr younger than the low mass ones. In an attempt to improve these values, we present in this paper deep $uvby\beta$ photometry of the double open cluster h & χ Persei. Given the nearness of these clusters, our magnitude limit ($V = 16.5$) allows us to reach early-F main sequence stars. This is 3 mag deeper than the previous study by Crawford et al. (1970b) and allows us a very accurate fit to the Zero Age Main Sequence (ZAMS) and hence precise determination of the astrophysical parameters of the clusters.

2. Observations

Observations of the central region of h & χ Persei were obtained at the 1-m Jacobus Kapteyn Telescope (JKT), located at the Observatorio del Roque de los Muchachos, La Palma, Spain on the nights of 10–22 December 1997. The telescope was equipped with the 1024×1024 TEK 4 chip CCD and the four Strömgren $uvby$ and the narrow and wide Hβ filters. Pixel size was $0''.331$ in such a way that the whole field covered by each frame was $5'.6 \times 5'.6$. Even though both clusters are actually more extended than the area covered by our frames ($\sim 18'$ across considering the outermost regions), our images are centered on the central region of both clusters, where member star density is much higher.

We took two frames covering the whole of the central region of each cluster (central coordinates are displayed in Table 1). Figures 1a,b show plots of the observed fields in h & χ Persei respectively. The dot sizes are indicative of the relative instrumental y magnitude. Each cluster was observed using three different exposure times in each filter (Table 1), so that the widest range of magnitudes possible was observed with good signal-to-noise ratio. Standard stars were observed in the clusters h & χ Persei, NGC 6910, NGC 2169 and NGC 1039 using the intermediate exposure time.

Throughout this paper the numbering system used will be that of Oosterhoff (1937). For those stars that were not observed by Oosterhoff (1937), a new system has been

adopted. New stars in h Persei are listed after a "4" prefix, while new stars in χ Persei are listed starting with a "7" prefix. Coordinates in each frame for these newly catalogued stars are given in Table 2.

It is worth noting that our sample is representative of the star population, except in the sense that it contains almost exclusively main-sequence stars (and some giants of the earlier spectral types). Most of the brightest member stars are far away from the central region. This has no bearing on the determination of the main cluster parameters (such as reddening and distance), but can influence the study of the system age. For this reason, we have supplemented our data with observations of a number of members brighter than $V = 11$ taken from Johnson & Morgan (1955) and Crawford et al. (1970b).

3. Reduction procedure

The reduction of all frames was carried out using the IRAF[1] routines for the bias and flat-field corrections. The photometry was obtained by PSF fitting using the DAOPHOT package (Stetson 1987) provided by IRAF. The atmospheric extinction corrections were performed using the RANBO2 program, which implements the method described by Manfroid (1993). It has been shown that the choice of standard stars for the transformation is a critical issue in $uvby\beta$ photometry. Transformations made only with unreddened stars introduce large systematic errors when applied to reddened stars, even if the colour range of the standards brackets that of the programme stars (Manfroid & Sterken 1987; Crawford 1994). Our data cover a very wide range of spectral types and hence a wide range of intrinsic colours. Moreover, during this campaign several clusters with different interstellar reddenings were observed.

In order to cover the whole range of programme stars, we selected our standard stars in the same clusters under investigation. A preliminary list of standard stars was built by selecting a number of non-variable non-peculiar candidate stars in h & χ Persei, NGC 2169, NGC 6910 and NGC 1039, observed with the same Kitt Peak telescopes and instrumentation used to define the *uvby* Crawford & Barnes (1970a) and Hβ Crawford & Mander (1966) standard systems, so that there is no doubt that the photometric values are in the standard systems. Since the original observations of h & χ Persei by Crawford et al. (1970b) do not include V values, we used values given by Johnson & Morgan (1955), which were also taken with the same instrumentation, for the V transformation.

The list of adopted standard stars and their photometric data to be used in the transformations are given in Tables 3 and 4.

The following *uvby* transformation equations from the instrumental to the standard system together with the standard errors on the coefficients are obtained using the equations by Crawford & Barnes (1970a), where the coefficients have been computed following the procedure described in detail by Grønbech et al. (1976):

$$V = 11.269 + 0.091(b-y) + y_{\rm i} \quad (1)$$
$$\pm 0.003 \quad \pm 0.007$$

$$(b-y) = 0.636 + 1.070(b-y)_{\rm i} \quad (2)$$
$$\pm 0.008 \ \pm 0.008$$

$$m_1 = -0.523 + 1.009 m_{1\rm i} - 0.206(b-y) \quad (3)$$
$$\pm 0.008 \quad \pm 0.015 \quad \pm 0.009$$

$$c_1 = 0.543 + 1.019 c_{1\rm i} + 0.257(b-y) \quad (4)$$
$$\pm 0.004 \ \pm 0.004 \quad \pm 0.007$$

where the index "i" stands for instrumental magnitudes.

The transformed values for the 41 standard stars are given in Table 5, together with their precision and deviation with respect to the published standard values. Table 6 shows the mean catalogue minus transformed values for the standard stars and their standard deviations, which constitute a measure of the accuracy of the transformation. From the mean differences between catalogue and transformed values, it is clear that there is not a significant offset between our photometry and the standard system. Since the individual differences for a few stars seem to be rather large, an attempt was made to improve the transformation by removing these stars from the standard list. We find however that the transformation coefficients and their precision do not improve significantly.

The Hβ instrumental system and transformation equations were computed following the procedure described in detail by Crawford & Mander (1966). The transformation coefficients are $a = 3.514$ and $b = 1.059$. Transformed values and their differences with respect to the mean catalogue values are given in Table 5. The mean difference is -0.003 with a standard deviation 0.031, which, as in the case of the *uvby* transformation, indicates that there is no significant offset with respect to the standard system.

4. Results

4.1. Membership and reddening

We have obtained $uvby\beta$ CCD photometry for more than 350 stars in the fields of h & χ Persei. The magnitude limit $V \approx 16.5$ allows us to identify 214 stars that were not catalogued by Oosterhoff (1937). Even though all of them are listed in Table 2 some of them are so faint that the number of counts was not enough to reach a good signal-to-noise ratio in all the filters. Therefore these stars are discarded from our sample.

To assess the membership of a star, we look at its position in the $V-(b-y)$ and $V-c_1$ diagrams. We find that in both diagrams the vast majority of the stars fall along a

[1] IRAF is distributed by the National Optical Astronomy Observatories, which are operated by the Association of Universities for Research in Astronomy, Inc., under contract with the National Science Foundation.

Table 3. Standard stars with their catalogued values and spectral types taken from the literature.

Number	V	$b-y$	m_1	c_1	β	*Spectral Type*
			h Persei			
837	14.080	0.393	0.000	0.918	2.801	
843	9.320	0.277	−0.050	0.166		B1.5V
867	10.510	0.393	0.161	0.375	2.613	
869					2.700	
935	14.020	0.362	−0.004	0.854	2.802	
950	11.290	0.318	−0.048	0.214	2.642	B2V
960					2.767	
978	10.590	0.305	−0.039	0.177	2.643	B2V–B1.5V
982					2.796	
1015	10.570	0.225	0.033	0.741		B8V
1078	9.750	0.316	−0.065	0.167	2.610	B1V–B1Vn
1181	12.650	0.372	−0.034	0.379	2.718	
			χ Persei			
2133					2.676	
2139	11.380	0.255	−0.033	0.196	2.649	B2V
2147	14.340	0.406	−0.050	1.002	2.863	
2167	13.360	0.352	−0.056	0.627	2.752	
2185	10.920	0.283	−0.049	0.406	2.700	B2Vn
2196	11.570	0.250	−0.006	0.210	2.670	B1.5V
2200					2.721	
2232	11.110	0.292	−0.105	0.207	2.651	B2V
2235	9.360	0.316	−0.088	0.150	2.611	B1V
2251	11.560	0.302	−0.042	0.349	2.709	B3V
			NGC 2169			
11	10.600	0.084	0.065	0.541	2.698	B8V
15	11.080	0.130	0.109	0.944	2.864	B9.5V
18	11.800	0.115	0.105	0.912	2.872	B9.5V

Table 4. Standard stars with their catalogued values and spectral types taken from the literature (continued Table 3).

Number	V	$b-y$	m_1	c_1	β	*Spectral Type*
			NGC 6910			
7	10.360	0.670	−0.160	0.110	2.612	B0.5V
11	10.900	0.770	0.420	0.430	2.555	
13	11.720	0.660	−0.140	0.220	2.647	B1V
14	11.730	0.590	−0.100	0.220	2.652	B1V
15	12.220	0.590	−0.110	0.330	2.679	
17	12.660	0.670	−0.120	0.310	2.659	
18	12.810	0.750	−0.140	0.290	2.680	
19	12.920	0.640	−0.120	0.380	2.662	
20	12.980	0.610	−0.130	0.420	2.692	
			NGC 1039			
92	11.960	0.303	0.138	0.481	2.678	
96	9.740	0.086	0.176	0.973	2.890	
97	11.820	0.144	0.198	0.900	2.855	
102	10.760	0.151	0.194	0.894	2.848	
105	11.220	0.176	0.204	0.796	2.817	
109	10.030	0.066	0.152	1.013	2.916	
111	9.950	0.055	0.163	1.021	2.908	

The data are taken from Crawford et al. (1970b) and Johnson & Morgan (1955) for h & χ Persei, Perry et al. (1978) for NGC 2169, Crawford et al. (1977) for NGC 6910 and Canterna et al. (1979) for NGC 1039. Spectral types, when available, are taken from Schild (1965) and Slettebak (1968) for h & χ Persei, Perry et al. (1978) for NGC 2169, Morgan & Harris (1956) and Hoag & Applequist (1965) for NGC 6910 and Canterna et al. (1979) for NGC 1039.

Table 5. Catalogue of 41 standard stars observed and transformed to the Crawford-Barnes $uvby$ and the Crawford-Mander Hβ standard systems. The internal rms errors of the mean measure in the transformation of each star are given in Cols. 8 to 11 in units of 0.001 mag. Columns 12 to 16 give the difference D = standard value minus transformed value, in units of 0.001 mag. N is the number of measures of each standard star in the transformation in V, $(b-y)$, m_1, c_1. The number of measures in β is one for each standard star in the transformation.

Star	V	$(b-y)$	m_1	c_1	β	N_{uvby}	σ_V	σ_{b-y}	σ_{m_1}	σ_{c_1}	D_V	$D_{(b-y)}$	D_{m_1}	D_{c_1}	D_β
						h Persei									
869	-	-	-	-	2.724	-	-	-	-	-	-	-	-	-	−024
837	14.095	0.411	−0.031	0.907	2.789	3	006	009	024	024	−016	−019	032	011	012
843	9.330	0.319	−0.151	0.240	-	1	-	-	-	-	−010	−042	101	−074	-
867	10.572	0.376	0.177	0.379	2.666	5	006	008	013	025	−063	016	−015	−005	−053
935	14.051	0.411	−0.076	0.856	2.781	6	018	007	018	038	−031	−049	073	−003	021
950	11.297	0.337	−0.079	0.221	2.630	1	-	-	-	-	−007	−019	031	−007	012
960	-	-	-	-	2.727	-	-	-	-	-	-	-	-	-	040
978	10.646	0.328	−0.070	0.194	2.634	5	016	013	016	023	−056	−023	031	−017	009
982	-	-	-	-	2.779	-	-	-	-	-	-	-	-	-	017
1015	10.573	0.223	0.029	0.677	-	2	037	023	006	030	−003	003	005	064	-
1078	9.775	0.317	−0.043	0.138	2.611	3	008	021	042	036	−025	−002	−021	030	−001
1181	12.655	0.352	−0.008	0.338	2.703	6	022	022	044	030	−006	020	−025	041	015
						χ Persei									
2133	-	-	-	-	2.658	-	-	-	-	-	-	-	-	-	018
2139	11.351	0.298	−0.097	0.235	2.641	2	011	024	030	007	029	−043	064	−039	008
2147	14.359	0.392	−0.083	1.022	2.783	5	023	034	051	051	−019	013	033	−020	080
2167	13.364	0.347	−0.080	0.616	2.733	6	012	008	012	024	−004	005	025	011	019
2185	10.926	0.275	−0.018	0.412	2.688	3	008	013	038	044	−006	008	−031	−006	012
2196	11.549	0.304	−0.066	0.246	2.632	6	012	013	023	023	021	−052	056	−034	038
2200	-	-	-	-	2.707	-	-	-	-	-	-	-	-	-	014
2232	11.052	0.238	−0.029	0.177	2.639	4	013	013	041	035	058	054	−077	030	012
2235	9.365	0.311	−0.071	0.131	2.575	3	012	015	046	039	−005	005	−016	018	036
2251	11.563	0.297	−0.028	0.367	2.689	6	009	011	027	030	−004	004	−013	−018	020
						NGC 2169									
11	10.538	0.076	0.061	0.545	2.719	1	-	-	-	-	062	008	004	−004	−021
15	11.023	0.122	0.092	0.939	2.856	1	-	-	-	-	057	008	017	005	008
18	11.733	0.053	0.260	0.813	2.883	1	-	-	-	-	067	062	−155	099	−011
						NGC 6910									
7	10.320	0.667	−0.150	0.092	2.652	2	011	004	012	016	041	003	−011	018	−040
11	-	-	-	-	2.639	-	-	-	-	-	-	-	-	-	−084
13	11.681	0.619	−0.082	0.211	2.661	2	004	023	038	004	039	041	−058	009	−014
14	11.730	0.569	−0.053	0.201	2.678	2	004	028	040	018	001	021	−048	019	−026
15	12.193	0.609	−0.134	0.359	2.698	2	007	006	014	002	027	−019	024	−029	−019
17	12.635	0.700	−0.149	0.294	2.688	2	008	010	025	040	025	−030	029	017	−029
18	12.816	0.755	−0.132	0.296	2.705	2	014	004	006	048	−006	−005	−009	−006	−025
19	12.897	0.610	−0.065	0.402	2.709	2	025	035	037	047	023	031	−056	−022	−047
20	12.920	0.619	−0.118	0.446	2.730	2	016	001	019	006	060	−009	−013	−026	−038
						NGC 1039									
92	11.928	0.282	0.150	0.520	2.709	1	-	-	-	-	032	021	−012	−039	−031
96	9.703	0.063	0.219	0.976	2.887	1	-	-	-	-	037	023	−043	−003	003
97	11.782	0.129	0.215	0.934	2.838	1	-	-	-	-	038	015	−017	−034	017
102	10.724	0.150	0.193	0.893	2.851	1	-	-	-	-	036	001	001	001	−003
105	11.166	0.167	0.232	0.971	2.832	1	-	-	-	-	054	009	028	−175	−015
109	10.034	0.040	0.178	1.018	2.960	1	-	-	-	-	−004	026	−026	−005	−044
111	9.900	0.025	0.249	0.964	2.927	1	-	-	-	-	050	030	−086	057	−019

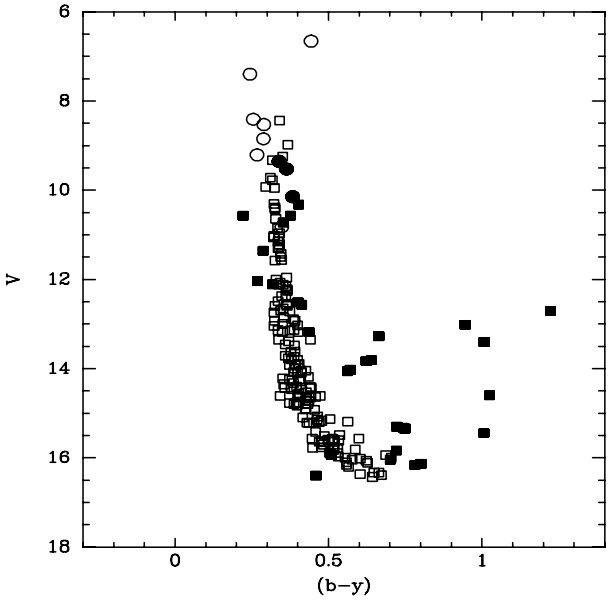

Fig. 2. $V-(b-y)$ diagram for all stars in the field of h Persei. Open squares represent stars considered as members while filled squares are non-members. Filled circles are stars catalogued as Be stars. Open circles are supergiant and giant stars not observed by us and taken from the study of Crawford et al. (1970b).

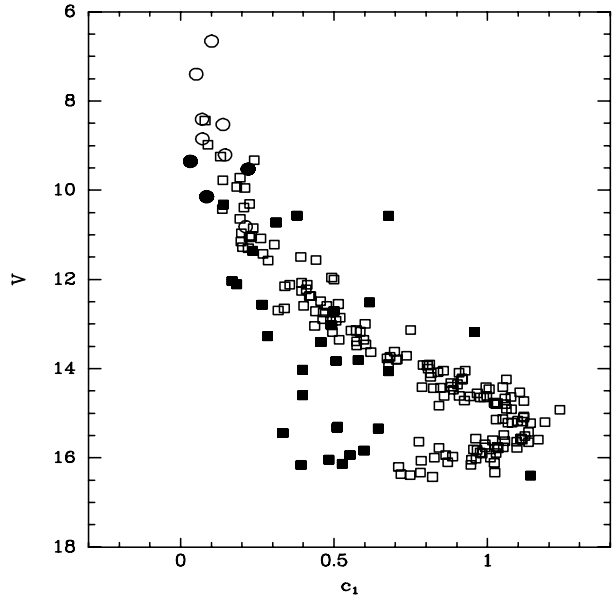

Fig. 3. $V-c_1$ diagram for all stars in the field of h Persei. Open squares represent stars considered as members while filled squares are non-members. Filled circles are stars catalogued as Be stars. Open circles are supergiant and giant stars not observed by us and taken from the study of Crawford et al. (1970b).

very well defined main sequence. Inspection of these photometric diagrams reveals that a number of stars do not fit well the main sequence loci in both diagrams. Those objects are considered as non-members unless they are catalogued as Be stars (see Figs. 2–5). Indeed Be stars have colours differing from those of non-emission B stars due to additional reddening caused by the circumstellar envelope and tend to have redder $(b-y)$ and lower c_1 values than normal B stars (Fabregat et al. 1996). In addition, the M4.5Iab supergiant star RS Per (2417) is considered to be a cluster member.

There is a smaller number of stars whose position is displaced with respect to the main sequence in only one of these diagrams. For these stars we calculate the free reddening indices $[m_1]$, $[c_1]$ and $[u-b]$:

$$[m_1] = m_1 + 0.32(b-y) \quad (5)$$

$$[c_1] = c_1 - 0.20(b-y) \quad (6)$$

$$[u-b] = [c_1] + 2[m_1] \quad (7)$$

and use the $\beta-[u-b]$ diagram to roughly evaluate their spectral classification (See Fig. 6). We find that stars 867, 969, 1084 and 1138 in h Persei and stars 2376, 7029 and 7081 in χ Persei have spectral types not corresponding to their photometric positions. We consider these objects as non-members. As the c_1 index is less affected by extinction than the $(b-y)$ colour, the $V-c_1$ diagram provides a more secure diagnostic than the $V-(b-y)$ diagram. Therefore, stars whose position only deviates from the main sequence in the $V-(b-y)$ plane could be affected by differential extinction. In χ Persei, the only case is star 2370. Since Muminov (1980) gives it a relatively low membership probability (0.38), we have excluded this star from further analysis. In h Persei, we have stars 911, 1072 and 1257. The membership probability is low for 911 and 1257 (0.15 and 0.36 respectively according to Muminov 1980). So we consider them as likely non-members of the cluster. Star 1072, on the other hand, has much higher probability, 0.78 (Muminov 1980), and we consider it a cluster member. Other stars, 2185, 2140 and 2311 in χ Persei have positions in the $V-c_1$ diagram deviating sligthly towards brighter V. The membership probability is high for 2185 and 2140 (0.76 and 0.98 respectively in Muminov 1980). We consider 2185 and 2140 as members. The case for 2311 is not so clear, but since it is likely to be an eclipsing binary (Krzesiński & Pigulski 1997), we will not use it for the determination of the cluster parameters, though it may well be a member (Vrancken et al. 2000). A similar situation occurs with the stars 859, 869, 926 and 1000. In h Persei we consider as non-member the star 859, because of its low membership probability (0.07; Muminov 1980), and as members stars 869, 926 and 1000 because of their higher probabilities (0.74, 0.60 and 0.99 respectively; Muminov 1980). In Tables 8 and 9 we present the resulting values for $V, (b-y), m_1, c_1$ and β and their precisions, together with the number of observations for member stars of h & χ Persei respectively. In Tables 10 and 11, we list the stars identified as non-members in the fields of h & χ Persei respectively together with their photometric data. Finally in Tables 12 and 13, we give the photometric data for Be star members of h & χ Persei respectively.

From the list of member stars we select those falling in

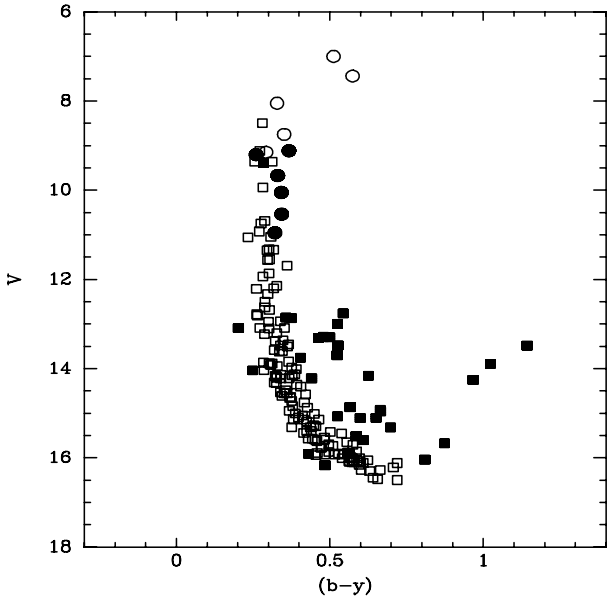

Fig. 4. $V-(b-y)$ diagram for all stars in the field of χ Persei. The open squares are considered as members and the filled squares as non-members. The filled circles are stars catalogued as Be stars. Open circles are supergiant and giant stars not observed by us and taken from the study of Crawford et al. (1970b).

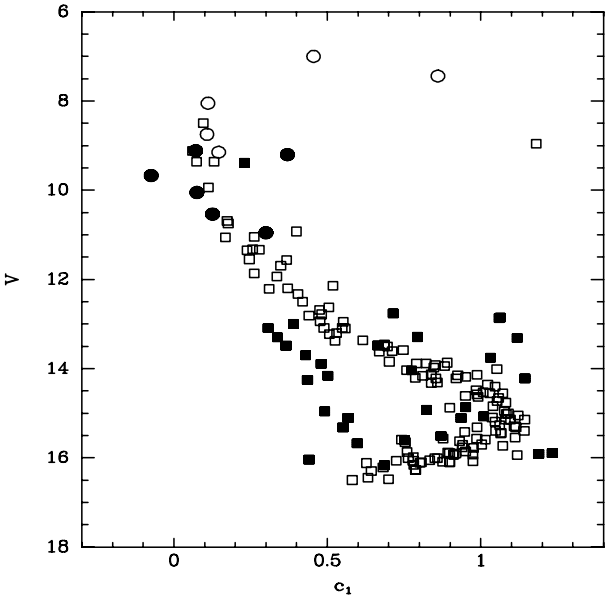

Fig. 5. $V-c_1$ diagram for all stars in the field of χ Persei. The open squares are considered as members and the filled squares as non-members. The filled circles are stars catalogued as Be stars. Open circles are supergiant and giant stars not observed by us and taken from the study of Crawford et al. (1970b).

Table 6. Mean catalogue minus transformed values for the standard stars and their standard deviations in V, $(b-y)$, m_1, c_1 and β.

D_{mV}	$D_{m(b-y)}$	D_{mm_1}	D_{mc_1}	$D_{m\beta}$
0.014	0.003	−0.005	−0.004	−0.003
0.033	0.027	0.049	0.044	0.031

the range of B-type stars in the $V-(b-y)$ and $V-c_1$ diagrams. From this subset we remove all Be stars and all early B stars which deviate strongly from the ZAMS. We also exclude stars 869, 926, 976, 1000, 1072, 2140 and 2185 because, in spite of appearing as likely members in the photometric diagrams, they have positions deviating slightly from the average loci of stars with the same spectral type. For all the remaining B stars we calculate individual reddenings. We follow the procedure described by Crawford et al. (1970b): we use the observed c_1 to predict the first approximation to $(b-y)_0$ with the expresion $(b-y)_0 = -0.116 + 0.097c_1$. Then we calculate $E(b-y) = (b-y) - (b-y)_0$ and use $E(c_1) = 0.2E(b-y)$ to correct c_1 for reddening $c_0 = c_1 - E(c_1)$. The intrinsic color $(b-y)_0$ is now calculated by replacing c_1 by c_0 in the above equation for $(b-y)_0$. Three iterations are enough to reach convergence in the process. The final average values of reddening are $E(b-y) = 0.44 \pm 0.02$ for h Persei and $E(b-y) = 0.39 \pm 0.05$ for χ Persei. These values are consistent, within the errors, with both clusters having the same reddening in their central region.

In the $E(b-y)$ – V diagrams (see Figs. 7 and 8) we notice that the scatter of individual reddenings is quite small in both clusters, confirming the result obtained by Crawford et al. (1970b) of homogeneous reddening across the central region. With the aid of these values we calculate the intrinsic colours and magnitudes of the candidate members of both clusters, listed in Table 14.

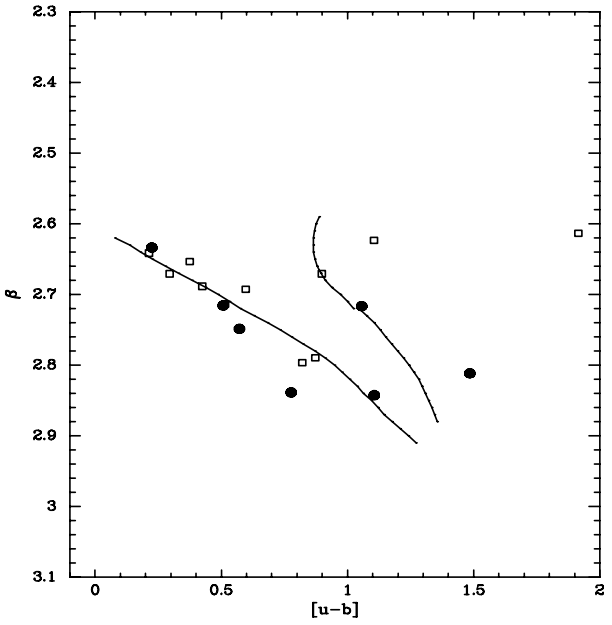

Fig. 6. $[u-b]-\beta$ diagram for all stars whose position deviates from the main sequence in only one of the photometric diagrams. The thin lines represent the loci of main-sequence B stars (left), the main sequence A-stars (bottom right) and the main sequence F-stars (top right). Open squares represent stars from the field of h Persei and while filled circles are from the field of χ Persei.

Table 7. Photometric data and spectral type for bright members of h & χ Persei taken from the literature. The fifth column indicates whether the star is inside the area covered by our observations (In) or more distant from the central region (Out).

h Persei						
Number	V	$(b-y)$	c_1	$E(b-y)$	*Position*	*Spectral Type*
3	7.400	0.244	0.051	0.360	Out	B2Ib
339	8.850	0.288	0.071	0.410	Out	B1IV
612	8.410	0.255	0.070	0.380	Out	B1II
1162	6.660	0.443	0.101	0.560	In	B2Ia
1187	10.820	0.348	0.212	0.460	In	B2IV
1899	8.530	0.289	0.138	0.400	Out	B2II
1781	9.210	0.267	0.145	0.380	Out	B1IV
χ Persei						
2227	8.050	0.328	0.111	0.440	In	B2II
2361	8.750	0.351	0.108	0.460	Out	B0.5III
2541	9.150	0.292	0.146	0.400	Out	B2II
2589	7.440	0.574	0.860	0.610	Out	A2Iap?
2621	7.000	0.512	0.455	0.590	Out	B8Ia

Since none of the stars in the sample, except RS Per, is in a late evolutionary state (all stars earlier than B3 deviate from the main sequence, but none seems to have a luminosity class higher than III), we have added to our colour-magnitude plots all the stars brighter than $V = 11$ taken from Johnson & Morgan (1955) and Crawford et al. (1970b), which, as shown in Sect. 3, are on the same system as our observations. Values of V (Johnson & Morgan 1955), $(b-y)$, c_1, individual $E(b-y)$, position in the clusters (Crawford et al. 1970b) and spectral type (Schild 1965; Slettebak 1968) are given in Table 7. A few of these stars are inside the area covered by our observations but were saturated in some of our frames.

As we can see from the values of individual reddening, the h Persei stars outside the inner 5.6 arcmin have reddenings lower that the average calculated for the inner 5.6 arcmin, and therefore they lie to the left of the rest of the members in the $V-(b-y)$ diagram. This is due to the fact that the $(b-y)$ colour is more affected by reddening than the c_1 index. Their position in the $V-c_1$ diagram agrees well with the rest of the cluster, because this index is very little affected by reddening.

In χ Persei three stars outside the central region have reddenings higher than the average for the central region, and therefore they lie to the right of the rest of the stars in the $V-(b-y)$ plane. Once more their position in the $V-c_1$ diagram is compatible with the rest of the cluster. We conclude that the analysis of the $V-c_1$ diagram yields much firmer results than the analysis of the $V-(b-y)$ diagram, as the actual position of each star in the latter is modified by the difference between its individual reddening and the average value for the central region.

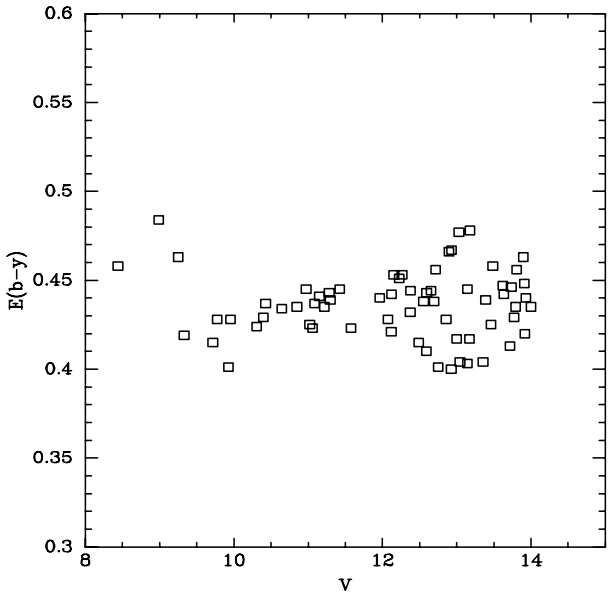

Fig. 7. Individual values of $E(b-y)$ calculated using Crawford's et al. (1970b) procedure against V magnitude for h Persei members in the B spectral type range.

4.2. Spectral classification

Given the paucity of spectroscopic studies of cluster members, we decided to estimate the spectral types for all members observed by us. Since our objects cover a wide range of spectral types, we use different procedures depending on the intrinsic photometric values. Following Napiwotzki et al. (1993), we select stars with $(b-y)_0 \leq 0.00$ (corresponding to $T_{\rm eff} \gtrsim 9500\,{\rm K}$) and use the temperature calibration based on the dereddened $[u-b]$ index, given by Napiwotzki et al. (1993):

$$\Theta \equiv \frac{5040\,{\rm K}}{T_{\rm eff}} = 0.1692 + 0.2828[u-b] - [u-b]^2. \qquad (8)$$

Once the temperature of the star is known, we derive an approximate value for the gravity $\log g$ by means of the grids of Moon & Dworetsky (1985). For the hottest stars ($T_{\rm eff} \gtrsim 20\,000\,{\rm K}$), only a rough estimate of $\log g$ is derived from the theoretical grids of Lester et al. (1986).

For stars with $0.00 \leq (b-y)_0 \leq 0.04$ (corresponding to $8500\,{\rm K} \lesssim T_{\rm eff} \lesssim 9500\,{\rm K}$), we use the parameters

$$a_0 = 1.36(b-y)_0 + 0.36m_0 + 0.18c_0 - 0.2448 \qquad (9)$$

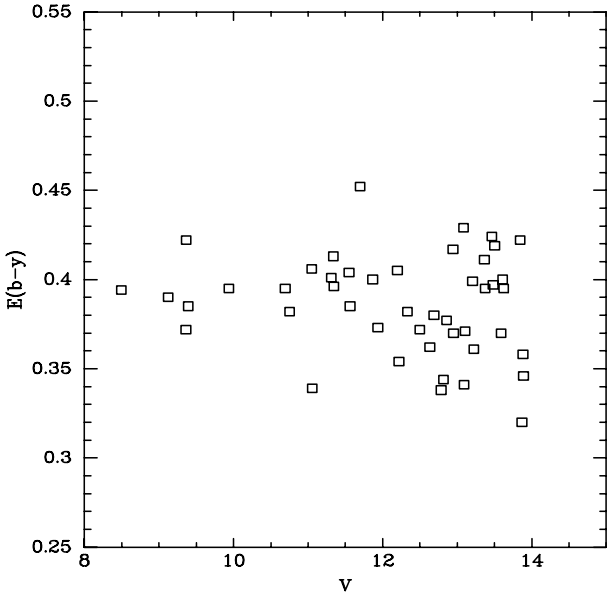

Fig. 8. Individual values of $E(b-y)$ calculated using Crawford's et al. (1970b) procedure against V magnitude for χ Persei members in the B spectral type range.

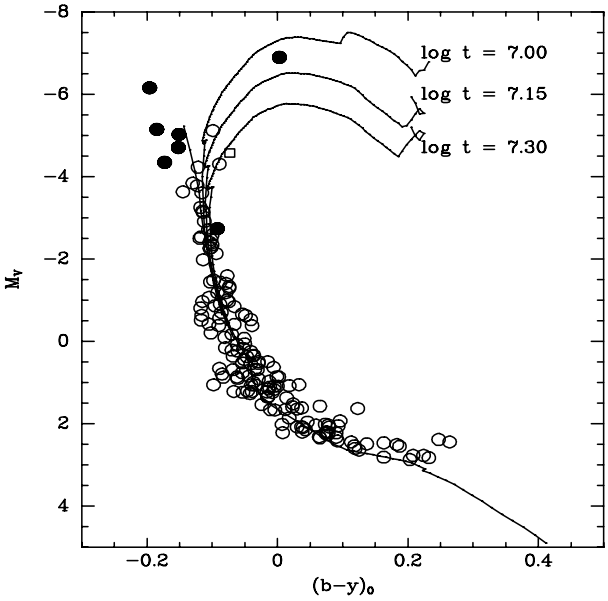

Fig. 9. Absolute magnitude M_V against intrinsic colour $(b-y)_0$ for h Persei members. The thick line represents the ZAMS from Perry et al. (1987). Three isochrones corresponding to $\log t = 7.0, 7.15$ and 7.30 are labelled with their respective $\log t$. Filled circles are supergiant stars not observed by us and taken from the study of Crawford et al. (1970b). Open squares are stars in our sample previously catalogued as having high rotational velocity (Slettebak 1968).

and

$$r^* = 0.35c_1 - 0.07(b-y) - (\beta - 2.565) \quad (10)$$

to derive both $T_{\rm eff}$ and $\log g$ from the grids of Moon & Dworetsky (1985).

Finally, for stars with $(b-y)_0 \geq 0.04$, we derive $T_{\rm eff}$ and $\log g$ directly from c_0 and β by using the grids of Moon & Dworetsky (1985).

As a last step, we derive approximate spectral types by correlating the estimated $T_{\rm eff}$ and $\log g$ with the average values for each spectral type from Kontizas & Theodossiou (1980) and Allen (1973). The estimated spectral types are listed in Table 14. The validity of this approximation is confirmed by the fact that, for all the stars which have a spectroscopic spectral classification, our estimate is consistent with the spectroscopic determination with an uncertainty of ±1 subtype. The only exception is the star 1116, for which we give a spectral type B2, while a spectral type B0.5V is given by Schild (1965). We note that, based on Geneva photometry, Waelkens et al. (1990) found that none of the stars classified as B0.5 in h Persei seems to be any hotter than other stars classified as B1 or B1.5, showing that the spectral classification of some stars is uncertain.

For the vast majority of the stars in the sample, we derive gravities compatible with their being main-sequence objects. Among the F and late A stars the scatter in the derived gravities is rather larger than among B-type stars, probably reflecting the larger errors associated with fainter magnitudes. For almost all of the stars at the low temperature end, we derive low gravities ($\log g \lesssim 3.6$). Among the stars later than F0, only 7097 (F4), 7108 (F2) and 7091 (F2) give $\log g \gtrsim 3.7$. The situation completely reverses for the hot stars. On the whole A0-F0 range, only star 856 (A7) has a value of $\log g$ that stands out as being particularly lower than that of all other stars. Among B stars, where the gravity determination is probably more reliable, a few stars have $\log g \approx 3.5$, and could be evolved. These are 1198 (B9), 1020 (B8), 1179 (B6) and 1232 (B3). From their atmospheric parameter calculations, Vrancken et al. (2000) find that B1 and B1.5 stars classified as main-sequence have gravities corresponding to higher luminosities. In particular, they find $\log g = 3.4$ for the star 2311 (B2III), for which we obtain $\log g \approx 3.5$. This would imply that also the star 2255 (B2) and the star 2246 (B1), for which we estimate a similar gravity, are giants.

4.3. Distance modulus determination

We have estimated the distance modulus to h & χ Persei by using both: (a) the β index calibration of Balona & Shobbrook (1984) and (b) by fitting the observed V_0 vs. $(b-y)_0$ and V_0 vs. c_0 ZAMS to the mean calibrations of Perry et al. (1987).

(a) Since the Balona & Shobbrook calibration is only valid for B-type stars, we select only those stars that we used for the reddening determination, calculate their intrinsic photometric indices adopting the average reddening for each cluster, and derive M_V from c_0 and β. For each star, we obtain the distance modulus $V_0 - M_V$, and finally we calculate the distance modulus for each cluster as the average of its members. The values obtained are listed in Tables 15 and 16.

Table 10. Photometric data for non-members of h Persei.

Number	V	$b-y$	m_1	c_1	β	σ_V	σ_{b-y}	σ_{m_1}	σ_{c_1}	σ_β	N_{uvby}	N_β
859	10.726	0.352	−0.126	0.311	2.642	0.018	0.015	0.024	0.021	0.004	5	2
865	13.276	0.663	0.538	0.283	2.577	0.015	0.012	0.021	0.023	0.013	4	3
867	10.572	0.376	0.177	0.379	2.671	0.006	0.008	0.013	0.025	0.007	5	2
886	15.346	0.749	−0.054	0.644	2.614	0.009	0.019	0.031	0.033	0.006	3	2
911	11.359	0.287	−0.033	0.235	2.671	0.013	0.010	0.015	0.009	0.010	4	2
969	13.017	0.945	0.100	0.490	2.624	0.008	0.017	0.039	0.016	0.019	5	3
1015	10.573	0.222	0.030	0.677	-	0.037	0.023	0.006	0.031	-	2	0
1023	12.567	0.413	0.197	0.266	2.659	0.021	0.016	0.030	0.018	0.005	5	3
1047	12.039	0.268	0.062	0.168	2.705	0.012	0.010	0.029	0.015	0.004	5	3
1054	13.831	0.623	0.111	0.506	2.606	0.017	0.010	0.021	0.045	0.026	6	3
1084	15.940	0.510	0.022	0.552	2.797	-	-	-	-	-	1	1
1099	13.179	0.436	−0.042	0.957	2.834	0.014	0.017	0.022	0.031	0.005	6	3
1100	14.060	0.562	0.094	0.677	2.761	0.030	0.041	0.102	0.084	0.018	6	3
1138	12.710	1.222	0.439	0.500	2.614	0.015	0.021	0.055	0.049	0.031	3	2
1155	12.518	0.400	−0.009	0.616	2.769	0.016	0.027	0.055	0.032	0.023	6	3
1167	14.028	0.571	0.129	0.398	2.628	0.032	0.020	0.054	0.044	0.013	6	3
1184	12.113	0.317	0.061	0.183	2.712	0.013	0.031	0.062	0.047	0.008	4	2
1189	13.810	0.639	0.147	0.579	2.615	0.016	0.012	0.069	0.165	0.027	4	2
1194	14.598	1.025	0.233	0.398	2.618	0.025	0.017	0.068	0.075	0.013	2	2
1238	15.324	0.743	0.003	0.510	2.656	-	-	-	-	-	1	1
1257	10.326	0.403	0.029	0.139	2.654	0.020	0.018	0.029	0.021	0.004	2	2
1272	13.406	1.007	0.179	0.457	2.604	0.016	0.023	0.030	0.015	0.028	2	2
4001	15.302	0.722	−0.001	0.512	2.650	0.012	0.003	0.011	0.054	-	3	1
4002	15.446	1.006	0.049	0.333	2.623	-	-	-	-	-	1	1
4007	15.838	0.721	−0.081	0.598	2.689	-	-	-	-	-	1	1
4014	16.044	0.701	−0.002	0.483	2.610	-	-	-	-	-	1	1
4019	16.135	0.801	−0.122	0.527	2.585	-	-	-	-	-	1	1
4021	16.162	0.782	−0.033	0.393	2.615	-	-	-	-	-	1	1
4040	16.400	0.459	−0.107	1.140	2.818	0.007	0.030	0.007	0.005	-	2	1

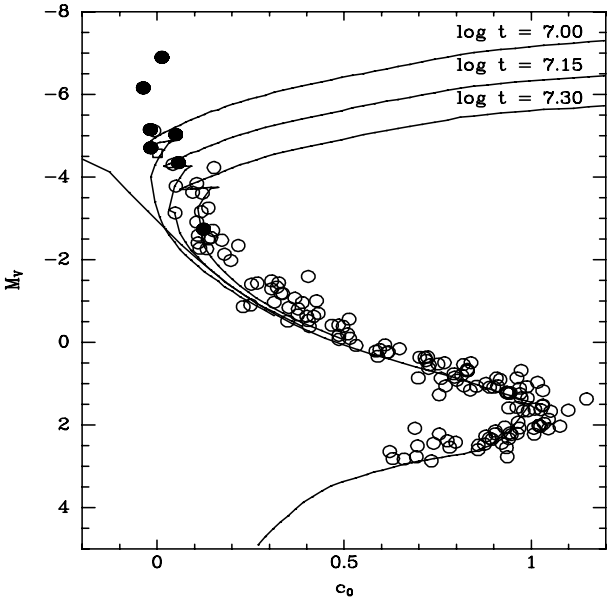

Fig. 10. Absolute magnitude M_V against intrinsic colour c_0 for h Persei members. The thick line represents the ZAMS from Perry et al. (1987). Three isochrones corresponding to $\log t = 7.0, 7.15$ and 7.30 are labelled with their respective $\log t$. Filled circles are supergiant stars not observed by us and taken from the study of Crawford et al. (1970b). Open squares are stars in our sample previously catalogued as having high rotational velocity (Slettebak 1968).

For h Persei, we find an average $V_0 - M_V = 11.4 \pm 0.5$, where the uncertainty represents only the standard deviation of the individual measurements and does not include the errors derived from the uncertainty in the photometric indices or the calibration itself. When these are taken into account, the determinations for all individual stars are compatible with the average value, but for the possible exception of star 880.

The average value for χ Persei is $V_0 - M_V = 12.1 \pm 0.2$. There are several stars that deviate considerably from the cluster mean, namely 2296, 2091 and 2251, some of which have very large uncertainties in M_V. Removing these stars does not significantly change the average value for $V_0 - M_V$. (b) Fitting the theoretical ZAMS is not only intrinsically more accurate, but also makes use of all the stars in the sample. This is important, because when the A and F stars are well fit to the ZAMS, it can be seen (Figs. 9–12) that *all* early B stars deviate significantly from the ZAMS.

We fit individually data from both clusters and derive best fit distance moduli of $V_0 - M_V = 11.56 \pm 0.20$ for χ Persei and $V_0 - M_V = 11.66 \pm 0.20$ for h Persei (the error indicates the uncertainty in positioning the theoretical ZAMS and its identification as a lower envelope). We see that the two values are, within the errors, identical, and that the values derived by using the Balona & Shobbrook calibration, with their larger errors, are compatible with

Table 11. Photometric data for non-members of χ Persei.

Number	V	$b-y$	m_1	c_1	β	σ_V	σ_{b-y}	σ_{m_1}	σ_{c_1}	σ_β	N_{uvby}	N_β
2087	13.315	0.463	0.002	1.119	2.851	0.003	0.029	0.045	0.048	0.013	3	3
2093	14.863	0.566	−0.060	0.951	2.831	0.025	0.012	0.038	0.022	0.036	3	2
2097	12.943	0.339	−0.058	0.476	2.699	0.018	0.020	0.028	0.030	0.006	6	4
2098	14.221	0.440	−0.040	1.144	2.891	0.012	0.031	0.044	0.051	0.012	4	3
2107	13.894	1.023	0.171	0.480	2.604	0.011	0.016	0.026	0.060	0.010	3	2
2127	14.961	0.666	0.016	0.491	2.612	0.026	0.020	0.019	0.039	0.004	3	2
2158	15.515	0.586	−0.025	0.870	0.000	-	-	-	-	-	1	0
2188	15.070	0.525	−0.036	1.010	2.861	0.018	0.037	0.056	0.029	0.018	3	2
2198	13.487	1.143	0.451	0.365	2.608	0.001	0.008	0.056	0.041	0.023	2	4
2202	13.300	0.500	0.142	0.337	2.629	0.023	0.025	0.027	0.019	0.013	3	3
2216	14.253	0.967	0.161	0.435	2.568	0.024	0.017	0.009	0.043	0.010	2	2
2281	15.110	0.599	−0.004	0.936	2.749	0.029	0.026	0.045	0.009	0.005	2	2
2315	13.754	0.404	−0.064	1.031	2.833	0.013	0.012	0.024	0.022	0.027	5	4
2329	12.762	0.543	0.111	0.714	2.657	0.018	0.022	0.046	0.050	0.005	6	4
2345	13.092	0.202	0.191	0.307	2.759	0.015	0.029	0.065	0.051	-	3	1
2356	15.104	0.651	−0.001	0.568	2.692	0.013	0.052	0.105	0.055	0.029	3	2
2365	13.701	0.524	0.072	0.430	2.620	0.033	0.035	0.063	0.038	0.018	6	4
2370	14.042	0.248	0.111	0.775	2.843	0.055	0.063	0.131	0.090	0.027	6	4
2376	13.481	0.526	0.080	0.665	2.717	0.023	0.034	0.081	0.039	0.030	6	4
2381	13.003	0.525	0.278	0.389	2.584	0.017	0.022	0.039	0.041	0.014	6	4
2397	14.161	0.625	0.036	0.502	2.649	0.029	0.023	0.072	0.032	0.041	5	4
7013	15.320	0.698	−0.005	0.551	2.601	-	-	-	-	0.041	1	2
7025	13.292	0.480	−0.011	0.793	2.777	-	-	-	-	-	1	1
7029	16.166	0.484	−0.061	0.686	2.839	-	-	-	-	-	1	1
7035	15.677	0.874	−0.161	0.598	2.596	-	-	-	-	-	1	1
7044	16.040	0.809	−0.110	0.440	2.610	-	-	-	-	-	1	1
7071	15.601	0.608	0.004	0.751	2.719	0.002	0.005	0.005	0.064	0.043	2	2
7081	15.899	0.564	0.002	1.233	2.812	-	-	-	-	-	1	1
7082	12.856	0.357	0.102	1.063	-	-	-	-	-	-	1	0
7101	15.912	0.431	0.024	1.188	2.907	0.042	0.011	0.016	0.036	2	1	

Table 12. Photometric data for Be stars of h Persei.

Number	V	$b-y$	m_1	c_1	β	σ_V	σ_{b-y}	σ_{m_1}	σ_{c_1}	σ_β	N_{uvby}	N_β
922	9.528	0.363	−0.188	0.220	2.600	0.008	0.004	0.015	0.008	-	2	1
1161	10.148	0.383	−0.047	0.085	2.559	0.019	0.021	0.046	0.036	0.001	5	2
1268	9.355	0.339	−0.019	0.032	2.624	0.008	0.001	0.008	0.019	-	2	1

Table 13. Photometric data for Be stars of χ Persei.

Number	V	$b-y$	m_1	c_1	β	σ_V	σ_{b-y}	σ_{m_1}	σ_{c_1}	σ_β	N_{uvby}	N_β
2088	9.117	0.367	−0.161	0.071	2.544	-	-	-	-	-	1	1
2165	10.053	0.342	−0.114	0.075	2.483	0.018	0.019	0.033	0.016	0.011	4	3
2242	10.956	0.321	−0.076	0.300	2.552	0.010	0.016	0.030	0.021	0.015	5	3
2262	10.538	0.343	−0.110	0.126	2.542	0.005	0.012	0.012	0.014	0.020	5	3
2284	9.673	0.330	−0.034	−0.074	2.426	0.013	0.017	0.070	0.072	0.019	3	2
2371	9.204	0.260	0.040	0.370	2.585	0.022	0.053	0.135	0.513	0.016	3	2

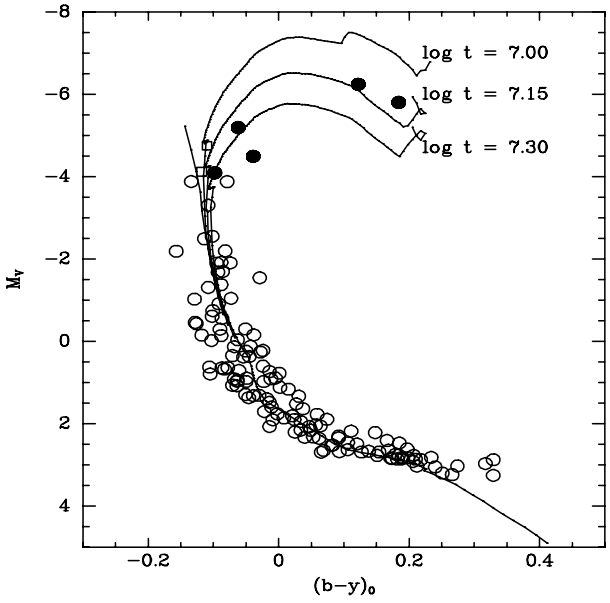

Fig. 11. Absolute magnitude M_V against intrinsic colour $(b-y)_0$ for χ Persei members. The thick line represents the ZAMS from Perry et al. (1987). Three isochrones corresponding to $\log t = 7.0, 7.15$ and 7.30 are labelled with their respective $\log t$. Filled circles are supergiant and giant stars not observed by us and taken from the study of Crawford et al. (1970b). Open squares are stars in our sample previously catalogued as having high rotational velocity (Slettebak 1968).

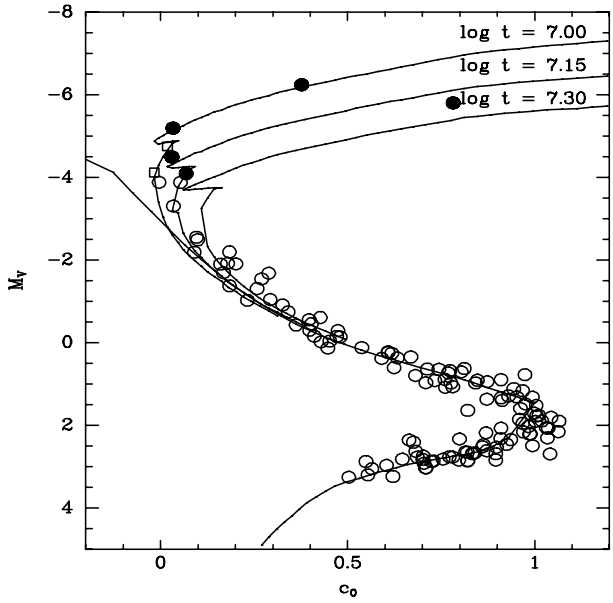

Fig. 12. Absolute magnitude M_V against intrinsic colour c_0 for χ Persei members. The thick line represents the ZAMS from Perry et al. (1987). Three isochrones corresponding to $\log t = 7.0, 7.15$ and 7.30 are labelled with their respective $\log t$. Filled circles are supergiant and giant stars not observed by us and taken from the study of Crawford et al. (1970b). Open squares are stars in our sample previously catalogued as having high rotational velocity (Slettebak 1968).

them. We therefore come to the conclusion that both clusters are indeed at the same distance.

As a further test, we plot in Figs. 13 and 14 the combined $V_0 - (b-y)_0$ and $V_0 - c_0$ diagrams for stars in both clusters. Points in these diagrams represent average values for the photometric index, taken over an interval of 0.5 mag, displaced by the individual distance modulus found for each cluster. It is obvious that both clusters fit the same ZAMS, confirming that the distance modulus are basically identical.

4.4. Age determination

(a) We first derive the age of both clusters on the basis of the data of our sample. It is well known that a number of giant stars in h & χ Persei have rotational velocities considerably higher than the average for field stars of the same spectral type and also that some of these are Be stars (Slettebak 1968; Waelkens et al. 1990; Denoyelle et al. 1994). Such stars can occupy positions in the photometric diagrams that differ considerably from those of non-peculiar stars of the same spectral type. For this reason, no Be stars have been included in our plots. Similarly, three supergiants binaries and four possible binary candidates in the clusters observed by Abt & Levy (1973) have also been excluded.

By comparing Figs. 13 and 14, it is obvious that the dispersion in the location of evolved stars in the $M_V - (b-y)_0$ diagram is an artifact introduced by differential reddening, since it disappears completely in the $M_V - c_0$ diagram. This again confirms that the latter must be preferred as the reference colour-magnitude plot.

Also plotted in Figs. 9–14 are isochrones computed with the evolutionary models of Schaller et al. (1992) for a log age of 7.00, 7.15 and 7.30 respectively (Meynet et al. 1993). The metallicities adopted are $X = 0.68$, $Y = 0.30$ and $Z = 0.020$ (Schaller et al. 1992). The isochrones have been transformed from the Log$T$-Log$L$ plane to the $uvby$ system after Torrejón (1996). The data clearly show that the main-sequence turnoff in h Persei occurs at a later spectral type than in χ Persei, which indicates that, contrary to previous speculations, h Persei is actually *older* than χ Persei.

In spite of this it is clear from Fig. 10 that the brightest stars in h Persei are substantially younger than the rest of the cluster, with some of them falling on the $\log t = 7.0$ isochrone. This effect cannot be due to the fact that some of the stars are fast rotators. In Figs. 9–12 stars with high rotational velocities have been identified (1133 in h Persei and 2296 and 2299 in χ Persei, Slettebak 1968). Most of the stars falling on the $\log t = 7.0$ isochrone have low measured rotational velocities. Morever Meynet & Maeder (2000) have shown that a $\log t = 7.3$ isochrone for high rotational velocity stars is almost identical to a $\log t = 7.2$ isochrone without rotation and therefore a variation in $\log t$ of 0.3 dex is too high to be explained by high rotation alone.

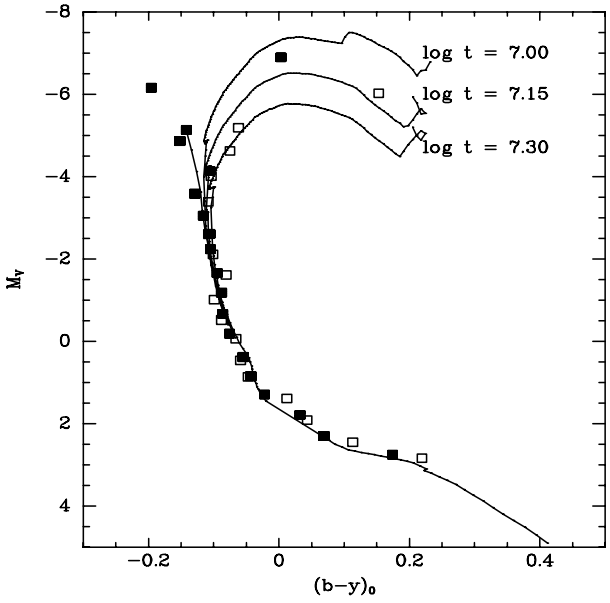

Fig. 13. Absolute magnitude M_V against intrinsic colour $(b-y)_0$ for h & χ Persei members. The ZAMS and isochrones are as in figures for the individual clusters. Data points represent averages taken over 0.5 mag intervals for each cluster. Filled squares are datapoints for h Persei, while open squares are datapoints for χ Persei.

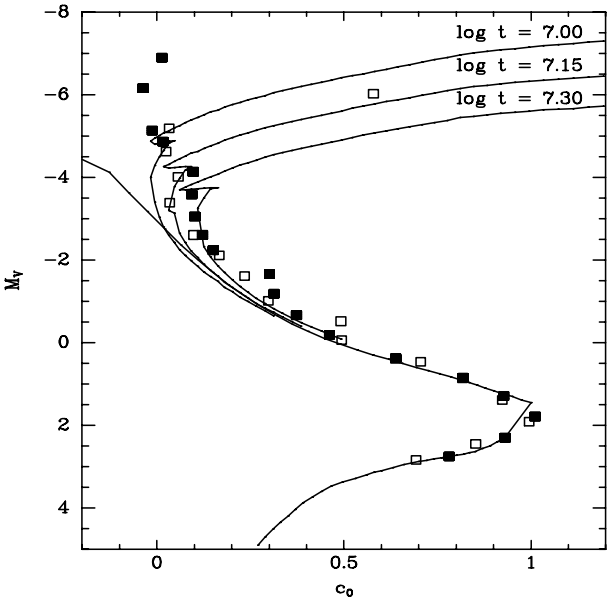

Fig. 14. Absolute magnitude M_V against intrinsic colour c_0 for h & χ Persei members. The ZAMS and isochrones are as in figures for the individual clusters. Data points represent averages taken over 0.5 mag intervals for each cluster. Filled squares are datapoints for h Persei, while open squares are datapoints for χ Persei.

(b) In order to verify our conclusions, we have included data for a few stars brighter than $V = 11$ taken from the literature, (see discussion in Sect. 4.1). For consistency, their unreddened photometric values have been calculated with the average reddening obtained for the central region of both clusters, since we have already shown that this has little bearing on the $M_V - c_0$ diagram.

Inclusion of brighter stars in the H–R diagram of h Persei corroborates our original finding. All the earliest stars are consistent with $\log t = 7.0$ or even younger, with the brightest supergiant stars even suggesting $\log t = 6.8$ (See Fig. 10).

This two-branch age distribution, with most stars being compatible with $\log t = 7.3$ and all the massive stars indicating $\log t = 7.0$ or younger is clearly not due to the presence of binaries or high rotational velocity stars.

The presence of stars with high rotation results in an apparent age dispersion (Meynet & Maeder 2000) and not in the separation into two branches. We note that massive stars from both the central region and the outskirts of the cluster display this effect without any obvious age separation, i.e., the younger age of massive stars does not seem to be related to their spatial distribution.

A similar situation can be observed in χ Persei (see Fig. 12). Two of the brightest stars seem to be younger than the rest of the cluster and fit the $\log t = 7.0$ isochrone. In this case, however, dispersion due to effects such as rotation cannot be ruled out, specially since not all bright stars seem younger than the bulk of the cluster.

5. Discussion

We find that the reddening and distance moduli to h & χ Persei are consistent with both clusters being placed at the same distance. However, the later main-sequence turnoff of h Persei indicates that this cluster is older than χ Persei, as far as a single age determination is meaningful. From isochrone fitting, we find that the bulk of stars in h Persei fit an age of $\log t = 7.30$, while in χ Persei no star seems to be old enough to lie on the $\log t = 7.30$ isochrone. However, all the earliest stars in h Persei deviate clearly and strongly from the rest of the cluster with some stars falling along the $\log t = 7.0$ isochrone and the brightest objects being even younger (probably as young as $\approx \log t = 6.8$).

Almost all the stars in χ Persei are consistent with $\log t = 7.10 - 7.15$, though two of the brightest stars could be slightly younger ($\log t = 7.00$). The low age of the few brightest members of h Persei is the reason why previous authors attributed a younger age to h Persei than to χ Persei (Tapia et al. 1984; Schild 1967). On the other hand, the age of most stars in χ Persei corresponds approximately to the average between the two branches in h Persei, which explains why other authors have given the same age for both clusters (Crawford et al. 1970b). The presence of at least two branches in the H–R diagram for h Persei strongly suggests two star formation epochs, the younger one corresponding to the more massive stars.

Since the age of the bulk of χ Persei does *not* correspond to any of the two isochrone fits in h Persei (which we find to be at the same distance), the evidence points to several stages of star formation in the region.

Table 14. Intrinsic photometric values and approximate spectral classification for all members (h Persei members on the left column, χ Persei members on the right). Unless otherwise indicated in the text, luminosity class is always taken to be V.

Number	V_0	$(b-y)_0$	c_0	Spectral Type	Number	V_0	$(b-y)_0$	c_0	Spectral Type
820	11.281	−0.090	0.497	B6	2085	9.648	−0.088	0.179	B3
821	13.600	0.096	0.965	A8	2091	10.022	−0.029	0.270	B3
832	12.325	−0.089	0.829	A0	2092	13.086	0.027	1.004	A2
836	13.883	0.008	0.754	A3	2094	10.189	−0.088	0.184	B2
837	12.203	−0.029	0.819	A0	-	-	-	-	-
842	11.250	−0.105	0.485	B7	2108	12.936	−0.046	0.872	A0
843	7.438	−0.122	0.152	B1	2109	13.340	0.059	1.005	A5
844	13.700	0.059	1.025	A8	2111	11.787	−0.024	0.608	B7
845	12.872	−0.046	0.934	A0	2114	9.369	−0.082	0.184	B2
848	13.203	−0.024	1.030	A2	2116	11.826	−0.028	0.618	B8
854	12.348	−0.035	0.973	A1	2123	13.376	0.021	1.044	A2
856	13.699	0.078	1.077	A7	2124	13.462	0.074	1.019	A5
857	13.017	−0.015	0.990	A0	2133	10.521	−0.073	0.293	B3
864	8.035	−0.145	0.095	B2	2139	9.661	−0.074	0.201	B1
875	13.719	0.093	0.929	A5	2147	12.682	0.002	0.944	A0
876	10.823	−0.066	0.352	B3	2149	12.456	−0.005	0.760	B9
879	9.686	−0.114	0.197	B2	2167	11.687	−0.043	0.538	B6
880	11.137	−0.041	0.404	B3	2170	13.621	0.064	1.031	A5
885	13.870	0.038	0.963	A5	2174	13.638	0.047	1.036	A7
892	9.324	−0.100	0.217	B1	2175	12.878	−0.030	0.952	A0
893	10.072	−0.077	0.404	B4	2179	12.462	−0.049	0.910	A0
896	10.597	−0.105	0.368	B5	2193	13.725	0.049	0.970	A5
898	12.660	−0.037	0.879	A0	2194	11.804	−0.050	0.608	B8
901	13.010	−0.015	0.973	A0	2196	9.872	−0.086	0.168	B2.5
907	10.482	−0.092	0.331	B3	2200	11.011	−0.087	0.397	B5
909	13.296	0.123	1.026	A7	2206	13.913	0.092	0.936	A7
914	13.310	0.030	1.099	A3	2209	13.719	0.034	1.063	A5
917	12.883	−0.067	0.935	A1	2211	11.273	−0.090	0.474	B7
923	11.152	−0.117	0.349	B5	2214	14.097	0.081	0.898	A7
924	13.281	0.037	1.010	A3	2215	13.869	0.092	1.034	A5
929	8.414	−0.118	0.137	B2	2219	13.746	0.111	0.870	A7
930	10.485	−0.079	0.336	B5	2223	12.341	0.001	0.974	A1
934	12.753	0.000	0.889	A0	2224	12.169	−0.024	0.624	B8
935	12.159	−0.029	0.768	B9	2229	9.666	−0.095	0.160	B2
936	8.503	−0.115	0.118	B1	2232	9.377	−0.157	0.090	B2
939	10.371	−0.074	0.306	B3	2235	7.688	−0.079	0.053	B1
941	13.325	−0.011	0.979	A1	2239	12.543	−0.023	0.776	B9
945	12.904	−0.053	0.942	A1	2240	12.359	−0.105	0.681	A0
946	12.526	−0.001	0.962	A1	2241	11.913	−0.071	0.669	B9
947	13.936	0.077	0.878	A7	2245	10.820	−0.101	0.341	B5
948	13.741	0.037	0.968	A3	2246	8.259	−0.108	0.034	B1
949	13.812	0.043	0.904	A5	2249	13.472	−0.009	1.002	A2
950	9.405	−0.104	0.133	B2	2251	9.886	−0.093	0.289	B4
952	10.180	−0.098	0.306	B3	2253	10.956	−0.102	0.427	B7
955	13.889	0.090	1.008	A8	2254	13.595	0.057	0.983	A5
956	10.662	−0.077	0.426	B5	2255	9.015	−0.102	0.096	B2
959	10.966	−0.086	0.431	B6	2258	12.271	−0.061	0.804	B9
960	11.823	−0.080	0.648	B9	2260	12.300	−0.014	0.769	B9
963	9.129	−0.117	0.144	B1	2261	12.857	−0.051	0.930	A0
965	10.703	−0.075	0.388	B5	2267	11.547	−0.103	0.429	B7
966	12.354	−0.068	0.830	A0	2268	11.945	−0.054	0.591	B8
970	12.511	−0.044	0.795	B9	2269	11.427	−0.088	0.480	B7
971	12.568	−0.061	0.917	A0	2270	12.476	−0.012	0.847	A0
978	8.754	−0.112	0.106	B2	2275	11.409	−0.038	0.411	B6
979	12.354	−0.031	0.829	A0	2277	13.271	−0.022	0.999	A2
980	7.824	−0.130	0.106	B1.5	2283	12.963	−0.018	0.913	A0
982	12.027	−0.068	0.702	B9	2286	13.048	−0.014	0.975	A1
985	10.226	−0.103	0.325	B4	2294	12.481	−0.068	0.733	B9

Table 14. continued.

Number	V_0	$(b-y)_0$	c_0	Spectral Type	Number	V_0	$(b-y)_0$	c_0	Spectral Type
986	10.697	−0.115	0.313	B5	2296	6.816	−0.110	0.018	B1.5
987	12.743	0.018	0.988	A3	2297	11.266	−0.051	0.398	B5
988	10.857	−0.118	0.377	B6	2299	7.447	−0.118	−0.01	B1
990	12.537	−0.083	0.759	A0	2300	13.921	0.062	0.664	–
991	9.535	−0.094	0.180	B2.5	2301	10.257	−0.108	0.258	B5
992	8.060	−0.116	0.121	B1.5	2307	13.518	0.034	0.968	A5
997	9.194	−0.102	0.173	B2	2309	11.107	−0.128	0.403	B7
999	11.462	−0.102	0.509	B8	2311	7.713	−0.106	0.152	B2
1004	8.957	−0.106	0.149	B2	2314	12.883	−0.039	0.994	A1
1007	13.683	0.007	1.021	A5	2317	13.328	−0.002	1.011	A2
1014	11.034	−0.116	0.400	B7	2319	11.415	−0.118	0.471	B8
1017	13.899	0.074	0.947	A8	2323	12.541	−0.050	0.842	A0
1018	13.761	0.039	1.046	A5	2324	12.212	−0.087	0.744	A0
1020	11.879	−0.070	0.585	B8	2331	12.508	−0.063	0.873	A0
1021	11.105	−0.089	0.513	B8	2332	12.901	0.031	0.910	A2
1025	13.859	0.075	0.943	A5	2335	12.729	0.015	0.968	A2
1028	12.886	−0.039	0.944	A1	2338	11.933	−0.045	0.633	B9
1030	14.156	0.137	0.859	A7	2349	11.138	−0.126	0.362	B7
1031	13.324	0.012	0.992	A3	2350	11.699	−0.068	0.447	B7
1034	13.254	0.023	0.940	A3	2352	10.655	−0.092	0.326	B6
1038	13.678	0.073	1.021	A5	2355	13.897	0.040	0.799	A5
1041	9.165	−0.119	0.136	B2.5	2358	12.631	−0.071	0.781	A0
1049	12.005	−0.036	0.590	B7	2359	12.205	−0.078	0.713	B9
1050	14.110	0.113	0.921	A7	2362	13.769	0.025	0.988	A3
1052	13.334	−0.004	1.052	A2	2363	12.243	−0.083	0.773	A0
1053	12.721	−0.098	0.771	A0	-	-	-	-	-
1056	12.779	−0.012	0.969	A0	2379	10.541	−0.129	0.232	B5
1058	11.729	−0.050	0.609	B8	2392	9.075	−0.114	0.099	B2
1059	12.836	−0.005	1.031	A1	2401	13.781	0.148	0.987	A5
1064	12.721	−0.040	0.820	A0	2407	12.647	−0.064	0.761	A0
1066	11.253	−0.066	0.467	B7	2410	12.533	−0.064	0.709	A0
1077	11.900	−0.061	0.618	B9	2414	12.192	−0.106	0.812	A2
1078	7.883	−0.123	0.050	B2	2416	13.636	−0.014	0.910	A3
1079	13.747	0.030	0.689	A2	7014	14.210	0.168	0.815	F0
1080	9.259	−0.104	0.109	B2.5	7015	14.253	0.154	0.833	A7
1081	12.428	−0.054	0.793	A0	7016	14.026	0.106	0.925	A5
1083	11.496	−0.070	0.486	B7	7017	14.486	0.206	0.7047	F3
1085	8.534	−0.114	0.048	B1.5	7021	14.594	0.274	0.708	F4
1091	13.986	0.064	0.888	A7	7023	14.383	0.234	0.755	A8
1093	11.594	−0.051	0.486	B7	7024	14.329	0.184	0.772	A8
1095	11.743	−0.062	0.532	B8	7027	14.036	0.185	0.863	F0
1096	13.186	0.024	1.031	A3	-	-	-	-	-
1105	12.107	−0.051	0.719	B9	7037	14.618	0.240	0.565	-
1106	12.212	−0.041	0.728	B9	7038	13.466	0.024	1.065	A2
1108	12.037	−0.047	0.716	B9	7045	13.975	0.166	0.676	F0
1109	9.080	−0.100	0.110	B3	7046	14.260	0.065	1.041	A8
1110	11.569	−0.081	0.515	B8	7047	14.425	0.182	0.821	A7
1116	7.360	−0.089	0.042	B2	7048	14.058	0.120	0.994	A5
1117	13.877	0.078	0.905	A8	7049	14.804	0.266	0.621	-
1118	12.193	−0.054	0.751	B9	7052	14.386	0.189	0.646	A7
1121	11.841	−0.052	0.595	B8	7054	14.392	0.198	0.701	F2
1122	10.332	−0.074	0.321	B6	7062	13.425	0.008	0.959	A2
1126	10.803	−0.096	0.230	B5	7064	14.255	0.127	0.896	F0
1128	10.261	−0.079	0.252	B5	7066	14.248	0.093	0.834	-
1129	11.038	−0.049	0.419	B7	7067	14.597	0.212	0.710	F5
1130	12.582	−0.029	0.801	A0	7068	14.233	0.138	0.840	A8
1132	6.548	−0.099	−0.00	B2	7070	14.441	0.218	0.724	F0
1133	7.095	−0.073	0.001	B1	7077	14.421	0.189	0.821	F0
1145	12.894	−0.016	0.937	A2	7080	14.182	0.197	0.872	A7

Table 14. continued.

Number	V_0	$(b-y)_0$	c_0	Spectral Type	Number	V_0	$(b-y)_0$	c_0	Spectral Type
1147	12.719	0.033	0.910	A3	7083	13.889	0.053	0.909	A7
1152	12.909	−0.008	0.970	A1	7084	11.529	−0.063	0.452	B7
1163	13.240	0.065	0.962	A7	7085	14.197	0.106	0.682	A7
1175	12.636	−0.013	1.017	A1	7086	7.684	−0.134	−0.00	B2.5
1179	11.003	−0.054	0.376	B6	7088	14.823	0.329	0.503	-
1180	12.937	−0.042	0.754	A2	7091	14.535	0.317	0.604	F2
1181	10.763	−0.088	0.250	B5	7092	13.162	−0.011	0.962	A2
1185	11.286	−0.039	0.407	B7	7093	14.337	0.151	0.686	F0
1190	13.527	0.018	1.046	A3	7096	14.310	0.179	0.702	A8
1191	12.821	−0.014	0.837	A0	7097	14.442	0.329	0.549	F4
1192	13.037	0.014	1.148	A3	7099	14.428	0.210	0.729	F2
1198	11.912	−0.041	0.615	B9	7104	14.086	0.083	0.861	A7
1202	10.231	−0.088	0.268	B5	7105	14.406	0.172	0.896	F0
1203	12.018	−0.038	0.723	B9	7108	14.766	0.251	0.554	F2
1206	12.754	−0.005	0.900	A1	7109	14.408	0.174	0.797	F0
1213	12.730	−0.034	0.854	A0	7116	14.334	0.207	0.781	F0
1218	13.997	0.090	0.940	A7	7118	14.216	0.069	0.820	A8
1222	13.747	0.079	1.007	A5	7122	13.204	0.037	0.821	A3
1232	9.391	−0.102	0.114	B3					
1240	14.013	0.065	0.895	A7					
1251	13.626	0.046	1.034	-					
1260	12.296	−0.006	0.726	A0					
1262	12.531	−0.062	0.907	A0					
1265	12.462	−0.085	0.814	A0					
1267	12.530	0.002	0.698	A0					
1281	12.159	−0.015	0.839	A0					
4009	14.050	0.247	0.776	A8					
4011	14.084	0.092	0.798	A7					
4012	14.108	0.264	0.739	F2					
4013	14.131	0.163	0.875	A8					
4016	14.171	0.183	0.696	F2					
4017	14.205	0.118	0.782	F0					
4018	14.216	0.187	0.934	A8					
4023	14.266	0.119	0.858	F0					
4025	14.309	0.125	0.622	F0					
4029	14.438	0.224	0.936	A7					
4030	14.438	0.208	0.693	-					
4036	14.480	0.163	0.630	F0					
4037	14.493	0.232	0.660	F0					
4042	14.538	0.203	0.733	F0					

This effect can be observed both when we consider only the stars covered by our observations (which are all relatively close to the main sequence) and also when the brighter members taken from the literature (in a later evolutionary stage and not necessarily belonging to the central region) are included. Since we have excluded any star that could be suspect of binarity or any pecularities, and the $M_V - c_0$ is not significatively affected by reddening, we may conclude that the age spread is real.

Our distance determination is consistent with some of the higher values found in literature (except those which give a different and larger distance to χ Persei). We derive our distance by fitting the ZAMS to stars much fainter than in previous work. As indicated by Vrancken et al. (2000), the lower distance moduli measured by Crawford et al. (1970b) and Balona & Shobbrook (1984) are due to their use of only the brightest stars. As can be seen in our HR diagrams, all stars earlier than ≈B3 deviate considerably from the ZAMS. This is again in agreement with the results of Vrancken et al. (2000), who find that all the stars in their sample of B1 and B2 stars are giants, even though some of them were previously classified as main-sequence.

From our data, we find no new Be stars in h & χ Persei. This is not the last word on this issue, because many catalogued Be stars do actually show a β index that does not indicate emission in our data. Since our census of B stars in the areas observed is complete, we can calculate the fraction of Be stars with respect to total number of B stars. In h Per, we find 3 Be stars among 74 B stars, which means an abundance $N_{\rm Be}/N_{\rm B+Be}$ (supergiants excluded) of 4%. In χ Persei, we find 6 Be stars out of 53 B stars, representing an abundance of 11%. Given the scatter in ages in h Per and the small number of Be stars, we cannot

Table 15. Individual intrinsic data for B stars in h (right) and χ (left) Persei. The colour excess $E(b-y)$ has been calculated using Crawford's et al. (1970b) procedure. The absolute magnitudes have been calculated by using the calibration (based on the β index) by Balona & Shobbrook (1984). The error in M_V has been computed using the formula by Balona & Shobbrook (1984). See text for details.

Number	$E(b-y)$	M_V	σ_{M_V}	V_0-M_V	Number	$E(b-y)$	M_V	σ_{M_V}	V_0-M_V
2085	0.401	−1.747	0.509	11.333	843	0.419	-	-	-
2091	0.452	−4.392	0.471	14.147	864	0.401	−2.224	0.298	10.259
2094	0.400	−1.858	0.252	12.003	876	0.456	−0.953	0.140	11.776
2111	0.424	−0.419	0.029	12.061	879	0.423	−2.051	0.273	11.737
2114	0.406	−2.223	0.131	11.521	880	0.477	−1.539	0.169	12.676
2116	0.419	−0.334	0.230	12.037	892	0.435	−2.015	0.542	11.339
2133	0.405	−1.401	0.263	11.858	893	0.440	−1.037	0.254	11.109
2139	0.413	−2.326	0.164	11.888	896	0.415	−1.384	0.405	11.981
2167	0.411	−0.377	0.103	11.972	907	0.432	−1.222	0.345	11.704
2194	0.397	−0.391	0.438	12.164	929	0.424	−2.647	0.120	11.061
2196	0.404	−2.135	0.252	11.947	930	0.444	−0.888	0.120	11.373
2200	0.380	−0.841	0.136	11.893	936	0.429	−2.673	0.090	11.176
2211	0.370	−0.916	0.365	12.276	939	0.453	−1.221	0.382	11.592
2224	0.422	−0.107	0.335	12.138	950	0.439	−2.533	-	11.938
2229	0.396	−2.228	0.312	11.870	952	0.428	−1.465	0.125	11.645
2232	0.339	−2.383	0.502	11.978	956	0.438	−0.919	0.087	11.581
2235	0.422	−3.839	0.968	11.387	959	0.428	−0.954	0.371	11.920
2241	0.370	0.109	0.388	11.892	963	0.425	−2.331	0.027	11.460
2245	0.372	−1.520	0.106	12.419	965	0.443	−0.844	0.493	11.547
2246	0.395	−3.555	0.904	11.794	978	0.434	−2.534	0.085	11.288
2251	0.385	−1.004	0.211	10.912	980	0.415	−2.788	0.280	10.612
2253	0.362	−0.496	0.426	11.572	985	0.421	−1.156	0.113	11.382
2255	0.395	−3.201	0.287	12.196	986	0.410	−1.280	0.078	11.977
2267	0.361	−0.300	0.199	11.972	988	0.401	−0.814	0.152	11.671
2268	0.395	−0.382	0.511	12.306	991	0.445	−2.224	0.131	11.759
2269	0.371	−0.560	0.280	12.068	992	0.428	−2.310	-	10.370
2275	0.429	−0.689	0.599	11.931	997	0.437	−2.023	0.146	11.217
2296	0.394	−3.855	0.825	10.652	1004	0.435	−2.327	0.107	11.284
2297	0.417	−1.003	0.108	12.153	1014	0.400	−0.442	0.386	11.476
2299	0.390	−3.860	0.292	11.308	1021	0.417	−0.085	0.254	11.190

derive any conclusions about the effect of cluster age on Be abundance.

6. Conclusions

We derive reddening and distance values consistent with the idea that h Persei and χ Persei are placed at the same distance. From the ZAMS fitting, we derive an approximate distance modulus $V_0 - M_V = 11.6 \pm 0.2$ for both clusters. The ages of the two clusters seem to be, however, different. There is evidence for two massive star populations in h Persei, fitting the $\log t = 7.0$ and $\log t = 7.3$ isochrones, with the more massive stars being younger. The age spread in χ Persei is, on the other hand, negligible, with all stars fitting the $\log t = 7.10 - 7.15$ isochrone. We interpret these data as favouring the idea that both clusters belong to a single star forming region in which at least three different star formation stages have taken place.

Acknowledgements. We would like to thank the Spanish CAT panel for allocating observing time to this project. AM would like to thank Dr. J. Fabregat for his help with the observations and Dr. J. M. Torrejón for making available the theoretical isochrones transformed to the M_V/c_0 and $M_V/(b-y)_0$ spaces. The authors gratefully acknowledge an anonymous referee for his/her very valuable comments.

Table 16. Individual intrinsic data for B stars in h (right) and χ (left) Persei. The colour excess $E(b-y)$ has been calculated using Crawford's et al. (1970b) procedure. The absolute magnitudes have been calculated by using the calibration (based on the β index) by Balona & Shobbrook (1984). The error in M_V has been computed using the formula by Balona & Shobbrook (1984). See text for details (continued Table 15).

Number	$E(b-y)$	M_V	σ_{M_V}	V_0-M_V	Number	$E(b-y)$	M_V	σ_{M_V}	V_0-M_V
2301	0.373	−1.185	0.371	11.516	1041	0.423	−2.199	0.406	11.364
2309	0.338	−0.935	0.123	12.266	1078	0.428	−3.191	0.035	11.074
2319	0.341	−0.590	0.299	12.214	1080	0.441	−2.284	0.102	11.543
2324	0.346	−0.095	0.091	12.496	1085	0.437	−2.839	0.090	11.373
2338	0.400	0.253	0.180	11.638	1109	0.445	−2.172	0.269	11.252
2349	0.344	−0.896	0.104	12.232	1116	0.463	−3.056	-	10.416
2350	0.395	−0.711	0.114	12.389	1122	0.451	−0.819	0.149	11.151
2352	0.382	−1.013	0.268	11.702	1126	0.438	−1.146	0.430	11.949
2359	0.358	0.487	0.144	11.855	1128	0.453	−1.487	0.330	11.748
2379	0.354	−1.367	0.157	12.064	1129	0.467	−0.642	0.175	11.680
2392	0.382	−2.142	0.383	11.250	1132	0.458	−4.037	-	10.585
2414	0.320	0.424	-	12.069	1133	0.484	-	-	-
7084	0.399	-	-	-	1179	0.466	−1.232	0.077	12.235
7086	0.372	−3.240	0.165	11.001	1181	0.444	−1.216	0.224	11.979
-	-	-	-	-	1202	0.442	−1.132	0.109	11.363
-	-	-	-	-	1232	0.443	−2.456	0.110	11.847

References

Abt, H. A., & Levy, S. G. 1973, ApJ, 184, 167
Allen, C. W. 1973, Astrophysical Quantities, 3rd ed. (London, Athlone)
Balona, L. A., & Shobbrook, R. R. 1984, MNRAS, 211, 375
Bidelman, W. P. 1943, ApJ, 98, 61
Canterna, R., Perry, C. L., & Crawford, D. L. 1979, PASP, 91, 263
Crawford, D. L. 1975a, AJ, 80, 955
Crawford, D. L. 1975b, PASP, 87, 481
Crawford, D. L. 1978, AJ, 83, 48
Crawford, D. L. 1994, PASP, 106, 397
Crawford, D. L., & Barnes, J. V. 1970a, AJ, 75, 978
Crawford, D. L., & Mander, J. 1966, AJ, 71, 114
Crawford, D. L., & Mandwewala, N. 1976, PASP, 88, 917
Crawford, D. L., Barnes, J. V., & Hill, G. 1977, AJ, 82, 606
Crawford, D. L., Glaspey, J. W., & Perry, C. L. 1970b, AJ, 75, 822
Denoyelle, J., Aerts, C., & Waelkens, C. 1994, in IAU Symp. 162, Pulsation, Rotation and Mass Loss in Early-Type Stars, ed. L. Balona, H. Heinrich, & J. M. Lecontel (Kluwer Academic Press, Holland), 151
Doom, C., De Greve, J. P., & De Loore, C. 1985, ApJ, 290, 185
Fabregat, J., Torrejón, J. M., Reig, P., et al. 1996, A&AS, 119, 271
Grønbech, B., Olsen, E. H., & Strömgren, B. 1976, A&AS, 26, 155
Hoag, A. A., & Applequist, L. 1965, ApJS, 12, 215
Johnson, H. L., & Morgan, W. W. 1955, ApJ, 122, 429
Kontizas, E., & Theodossiou, E. 1980, MNRAS, 192, 745
Krzesiński, J., & Pigulski, A. 1997, A&A, 325, 987
Lester, J. B., Gray, R. O., & Kurucz, R. L. 1986, ApJS, 61, 509
Manfroid, J. 1993, A&A, 271, 714
Manfroid, J., & Sterken, C. 1987, A&A, 71, 539
Mendoza, E. E. 1967, Bol. Obs. Tonantzintla y Tacubaya, 4, 149
Meynet, G., & Maeder, A. 2000, A&A, 361, 101
Meynet, G., Mermilliod, J. C., & Maeder, A. 1993, A&AS, 98, 477
Moon, T. T., & Dworetsky, M. M. 1985, MNRAS, 217, 305
Morgan, W. W., & Harris, D. L. 1956, Vistas Astron., 2, 1124
Muminov, M. 1983, BICDS, 24, 95
Napiwotzki, R., Schönberner, & Wenske, V. 1993, A&A, 268, 653
Oosterhoff, P. T. 1937, Ann. Sterrewatch Leiden, 17, 1
Perry, C. L., Lee, P. D., & Barnes, J. V. 1978, PASP, 90, 73
Perry, C. L., Olsen, E. H., & Crawford, D. L. 1987, PASP, 99, 1184
Schaller, G., Schaerer, D., Meynet, G., & Maeder, A. 1992, A&A, 96, 269
Schild, R. E. 1965, ApJ, 142, 979
Schild, R. E. 1966, ApJ, 146, 142
Schild, R. E. 1967, ApJ, 148, 449
Schild, R. E., & Romanishin, W. 1976, ApJ, 204, 493
Shobbrook, R. R. 1983, MNRAS, 205, 1215
Slettebak, A. 1968, ApJ, 154, 933
Stetson, P. B. 1987, PASP, 99, 191
Tapia, M., Roth, M., Costero, R., & Navarro, S. 1984, Rev. Mex. Astron. Astrofis., 9, 65
Torrejón, J. M. 1996, Tesina de Licenciatura, University of Valencia
Vrancken, M., Lennon, D. J., Dufton, P. L., & Lambert, D. L. 2000, A&A, 358, 639
Waelkens, C., Lampens, P., Heynderickx, D., et al. 1990, A&AS, 83, 11
Wildey, R. L. 1964, ApJS, 8, 439